Supporting Information

Chirality-controlled Spontaneous Twisting of Crystals *via* Thermal Topochemical Reaction

Rishika Rai[a,1], Baiju P. Krishnan[a,1] and Kana M. Sureshan[a,2]

[1]R.R and B.P.K. contributed equally to this work

[a] School of Chemistry, Indian Institute of Science Education and Research Thiruvananthapuram, Kerala 695551, India.

[2]Corresponding author. E-mail: kms@iisertvm.ac.in

S1. Materials and Methods

Chemicals and solvents were purchased from Sigma-Aldrich and were used without further purification. TLC analyses were carried out using precoated TLC silica gel 60 F_{254} plates purchased from Merck. Chromatograms were visualized under UV light and by dipping the plates into ceric ammonium molybdate staining solution followed by heating. NMR spectra were recorded on an Avance II-500 (Bruker) NMR spectrometer. IR spectra of samples were recorded by mixing with KBr and making pellet. Powder X-ray diffraction spectra were recorded using an X'pert PRO (PANalytics) powder diffractometer. For indexing the faces, a crystal was mounted on a Bruker platform goniometer with a CCD area detector and a video camera for viewing the crystal and unit cell of the crystal was measured. Bruker SMART software was used for crystal face indexing. DSC analyses were carried out using DSC Q20 differential scanning calorimeter, at a heating rate of 5 °C/min. Twisting nature of the crystals was observed using a Leica DM 2500 polarized light optical microscope, equipped with a Mettler Toledo FP82HT (temperature programmer) heating and freezing stage. Hot stage microscopy videos were recorded using LEICA DM 2500P Microscope and temperature control was done using Linkam temperature controller setup.

S2. Characterization of twisted crystals of LL

Comparison of IR spectra of twisted (old) and untwisted (fresh) crystals revealed that the relative intensity of the peak at 2103 cm^{-1}, characteristic of azide stretching band, is reduced in twisted crystals suggestive of partial consumption of the azide group, presumably due to a spontaneous TAAC reaction happening even at room temperature (Fig. S1A). Calorimetric studies earlier showed that the crystals of **LL** undergo an exothermic uncontrolled cycloaddition reaction at around 150 ˚C. Comparison of DSC profiles of twisted and untwisted crystals revealed that the heat liberated due to this uncontrolled reaction is reduced in twisted crystals (Figure S1B). This also suggests partial consumption of the dipeptide **LL** due to slow TAAC reaction at ambient conditions. ^{1}H NMR spectrum of twisted crystals proved that these crystals consisted of dipeptide **LL** and its 1,4-triazole-linked oligomers in 4:1 ratio (Fig. S1C). This clearly suggests that the dipeptide **LL** undergoes spontaneous azide-alkyne cycloaddition even upon storage for about a month at rt. The PXRD profile of twisted crystals showed the emergence of new peaks and preservation of crystallinity. The PXRD pattern of the twisted crystals was similar to that of

crystals of **LL** heated at 85 ˚C for 24 h, which is known to undergo TAAC reaction (Fig. S1D). These experiments prove that the crystals of **LL** undergo spontaneous topochemical reaction at room temperature and that the TAAC reaction is the cause of twisting of the crystals.

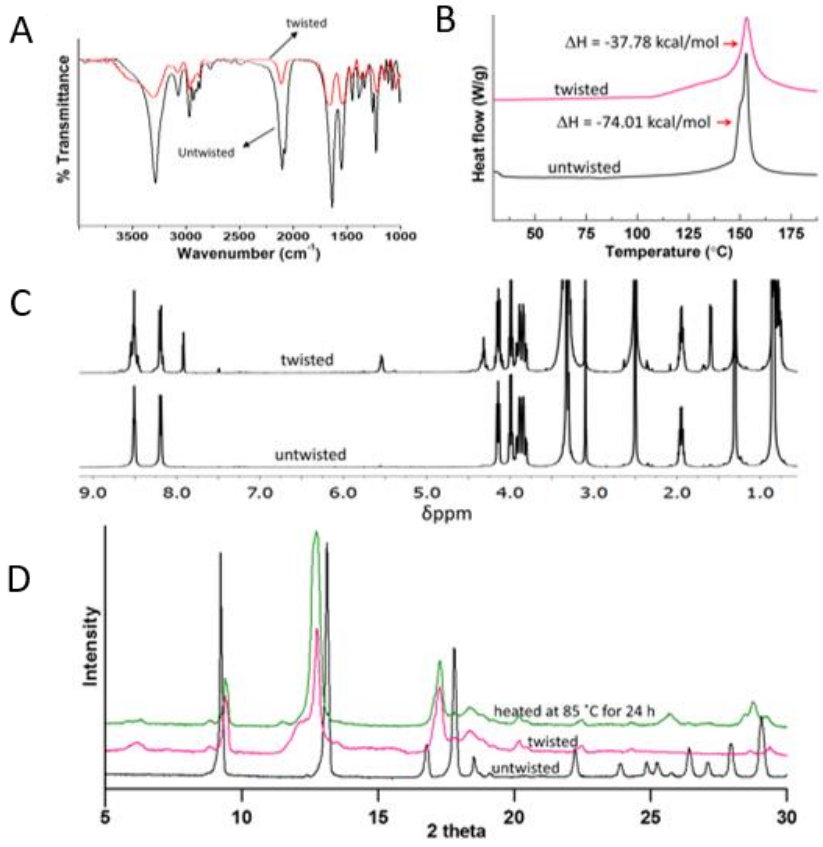

Fig. S1. (A) IR studies; (B) DSC profiles; (C) ^{1}H NMR spectral comparison of twisted and untwisted crystals; (D) Comparison of PXRD profiles of twisted and untwisted crystals with that of crystals which were heated at 85 ˚C for 24 h.

S3. Optical microscopy images

(A) Twisting of LL crystals after TAAC

We placed a crystal of the dipeptide **LL** on a glass plate and imaged using optical microscopy. Afterwards, the same crystal on the glass slide without changing its orientation was heated in a beaker which was a kept in an oil bath maintained at constant temperature of 85 ˚C. After heating for 3 days (heating at 85 ˚C for 3 days will complete TAAC), crystal was imaged again through

optical microscopy. The crystal showed twisted morphology suggesting topochemical reaction induced twisting of crystals (Fig. S2). We have repeated this experiment with different crystals.

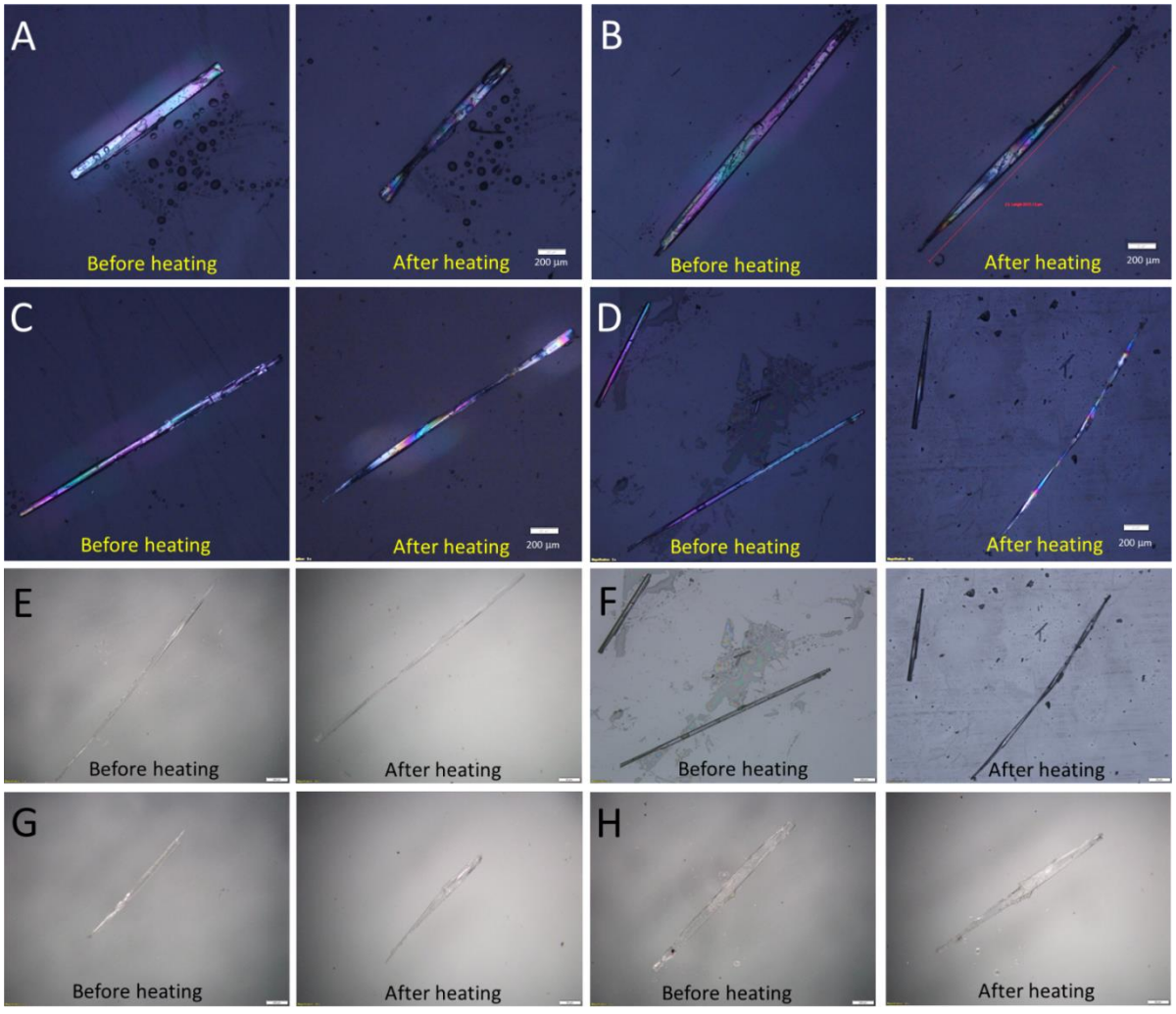

Fig. S2. Optical microscopic images of crystals of dipeptide **LL** before and after heating showing the twisted morphology in the reacted crystals; (A-D) with polarizer and (E-H) without polarizer. Scale bar: 200 µm.

(B) Hot-stage polarizing microscopy

We have picked several crystals of dipeptide **LL,** kept on a glass plate and observed under hot-stage polarizing light microscope. All the crystals were found to be defect-free under cross-polarized microscopy. Hot-stage polarized light microscopy images during heating also showed gradual twisting of the crystals suggesting topochemical reaction induced morphology change.

(C) Twisted crystals of LL after keeping in liq. N_2 bath

Cooling of the twisted crystals of the dipeptide **LL** to liquid nitrogen temperature did not show any untwisting, suggesting the irreversible nature of this mechanical response (Fig. S3). Also, heating-cooling cycle of twisted crystals in a differential scanning calorimeter confirmed the irreversible nature of this twisting. This is not surprising as the TAAC reaction, the basic process responsible for the mechanical response in the crystals of **LL** is irreversible. Materials that show irreversible mechanical response are useful as irreversible actuators for various important applications (1).

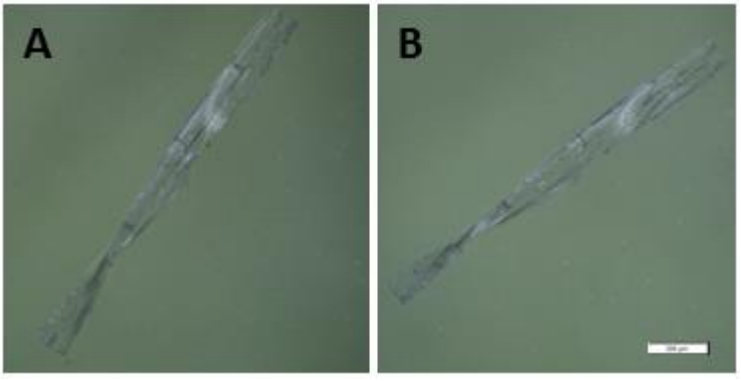

Fig. S3. Optical microscopic images of twisted crystal (A) before and (B) after keeping in liq. N_2 bath. Scale bar: 200 µm.

S4. ^{1}H NMR spectrum of LL crystals after heating till 90 ˚C

As the crystals twisted at 90 ˚C, we have recorded ^{1}H NMR spectrum of crystals after heating till twisting (90 ˚C). ^{1}H NMR spectrum revealed that about 10% reaction was completed by this time (Fig. S4). Yield of the reaction was found to be varying in the range of 5-10% from crystal to crystal. These results confirm that twisting is due to topochemical polymerization of dipeptide **LL**.

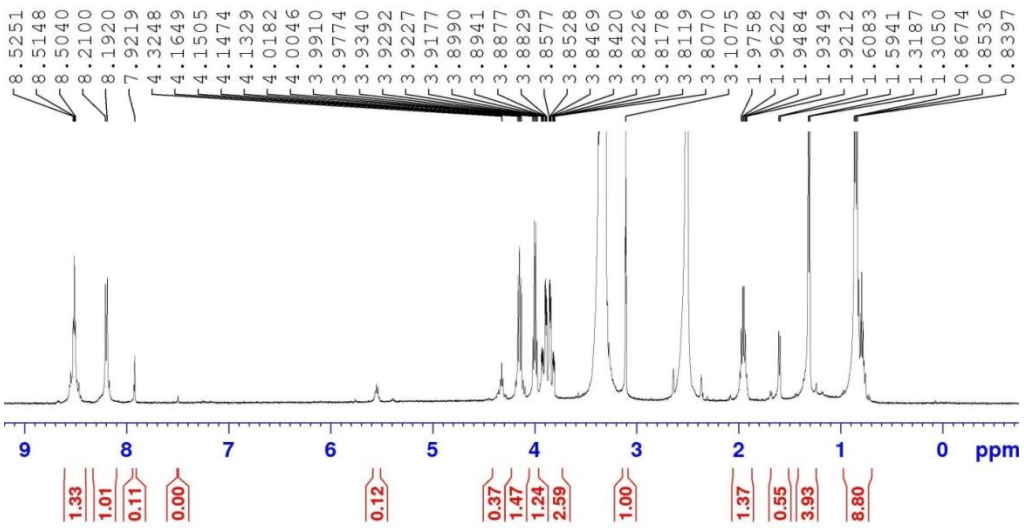

Fig. S4. ^{1}H NMR spectrum of crystals of the dipeptide **LL** heated till 90 ˚C.

S5. DSC experiment of LL crystals

DSC experiments were carried out with fresh crystals of dipeptide **LL** and twisted crystals which were obtained by heating fresh crystals till 90 ˚C and then cooled. DSC profiles of twisted crystals showed decrease in intensity of the exothermic peak (Fig. S5).

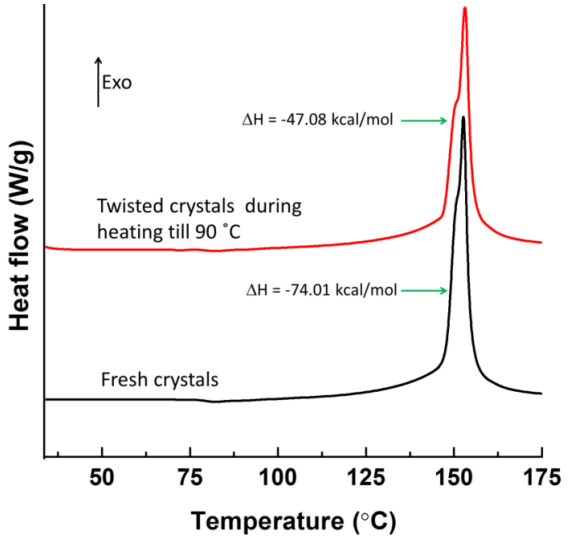

Fig. S5. DSC profile comparison of fresh **LL** crystals and preheated crystals (till 90 ˚C) after cooling to rt.

S6. IR study of LL crystals

IR spectra were also carried out with fresh crystals of dipeptide **LL** and twisted crystals which were obtained by heating the fresh crystals till 90 ˚C. IR spectrum showed that the relative intensity of azide stretching band was reduced. This also suggests the consumption of azide *via* topochemical polymerization by which, the twisting happened (Fig. S6).

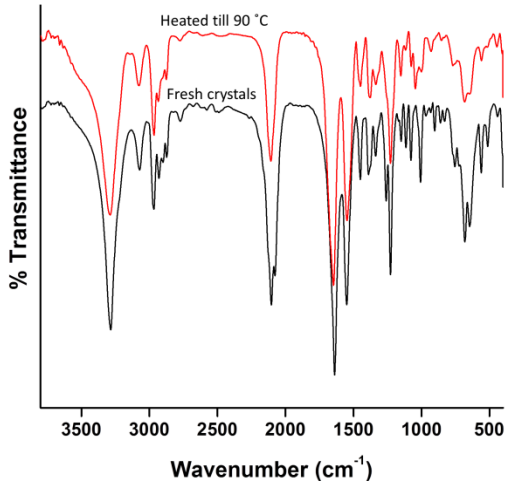

Fig. S6. IR spectral comparison of fresh **LL** crystals and twisted crystals which were obtained by heating till 90 ˚C.

S7. Crystal face indexing for LL crystal

Face indexing was done by mounting a long rectangular plate-like crystal on the goniometer. The length of the crystal is along crystallographic ‘b’ direction, the breadth is along ‘a’ direction and the height of the crystal coincides with the crystallographic ‘c’ direction. The (001) planes are the largest faces of the crystal, (100) planes are the second largest faces of the crystal and (010) planes intersects the crystal along its length.

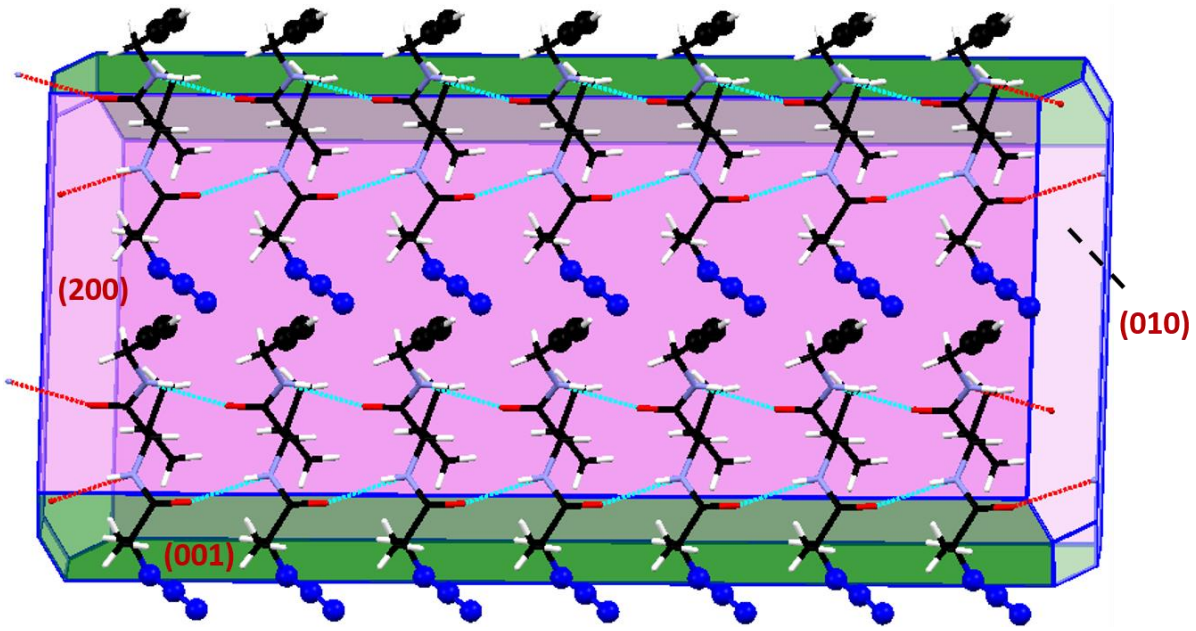

Fig. S7. BFDH morphology obtained (using Mercury, version 3.9) for crystal packing of **LL** (along bc plane), showing the direction of TAAC reaction along "c" axis (height of the crystal).

S8. Comparison of PXRD profiles of twisted LL crystals with that of untwisted crystals

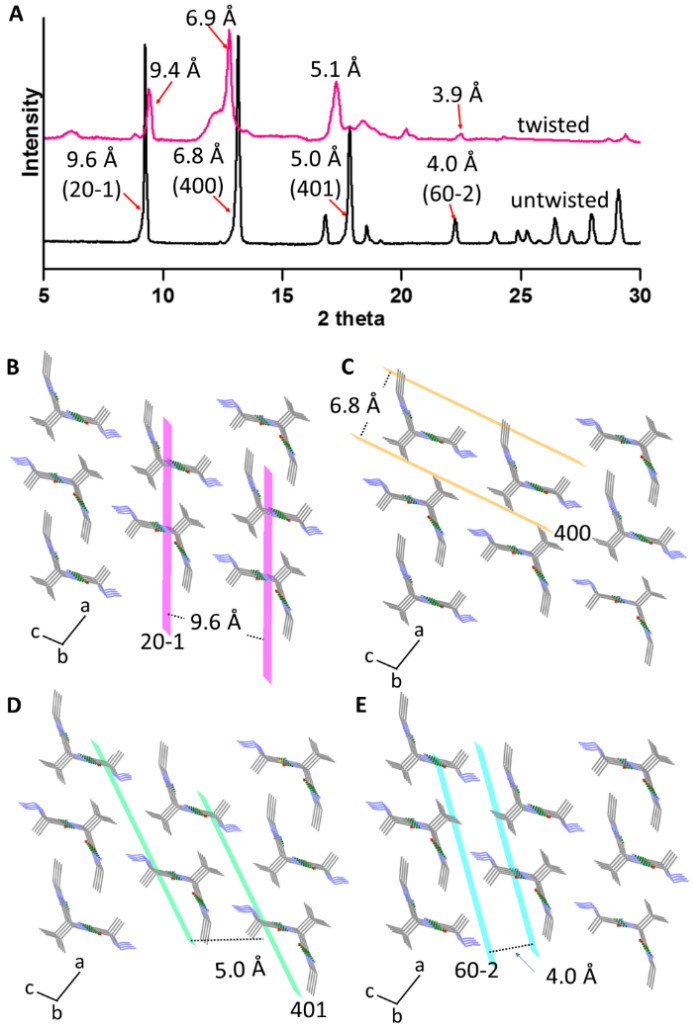

Fig. S8. (A) Comparison of PXRD peaks of twisted **LL** crystals with that of untwisted crystals; B-E) Images of various planes such as (20^{-}1), (400), (401) and (60^{-}2) respectively. The interplanar distance between (60^{-}2) and (20^{-}1) were found to decrease in the twisted crystals, due to the topochemical reaction along 'c' direction.

S9. Strain analyses

(A) Possible Factors influencing the strain in crystals

The usual cause for mechanical response is the generation of interfacial strain between daughter and parent domains. Elegant models have been proposed for various light-induced mechanical responses, including twisting (2). Similar general mechanism can be invoked in the present case

also. However, the reaction presented here is heat-induced reaction and is more complex. Various plausible contributors for the overall strain are:

(1) **Uneven stimulus**: When light is the stimulus, the irradiated surface will experience it uniformly. However, when heat is the stimulus, the heat-exposed surface of the crystal may experience uneven heating. This is because heat passes through a medium (contact between the hot-surface and crystal surface is equired) and crystal surfaces are often not perfectly planar and hence the extent of contact at different parts of crystal surface may vary (Fig. S9B).

(2) **Complex heterogeneity**: In usual reactive crystals, the reaction leads to a product and the interfacial strain between reacted and unreacted domains generate strain. But in the present case, the reaction leads to oligomers of different sizes and the heterogeneity is much more complex. Hence the interfacial strain can be more complex and different at different domains in the crystal (Fig. S9A).

(3) **Exothermic reaction**: The azide-alkyne cycloaddition is a highly exothermic reaction and hence releases a lot of energy to the crystal lattice. This energy released in the reaction also contribute to the over all strain (Fig. S9C).

(4) **Conformational Change**: The azide and alkyne motifs of adjacent reacting molecules are not-preorganized in a reactive (parallel) orientation. Hence the molecules have to undergo conformational change (rotation of alkyne and azide to reach parallel orientation) to reach reactive orientation. Interestingly along breadth of the crystal (a direction), the bc planes of molecules are aligned in oppposite direction. Thus the conformational changes (rotation) necessary for the reaction happen in opposite direction in adjacent planes. These conformational motion of molecules in opposite directions in adjacent planes may also contribute to the strain (Fig. S9D).

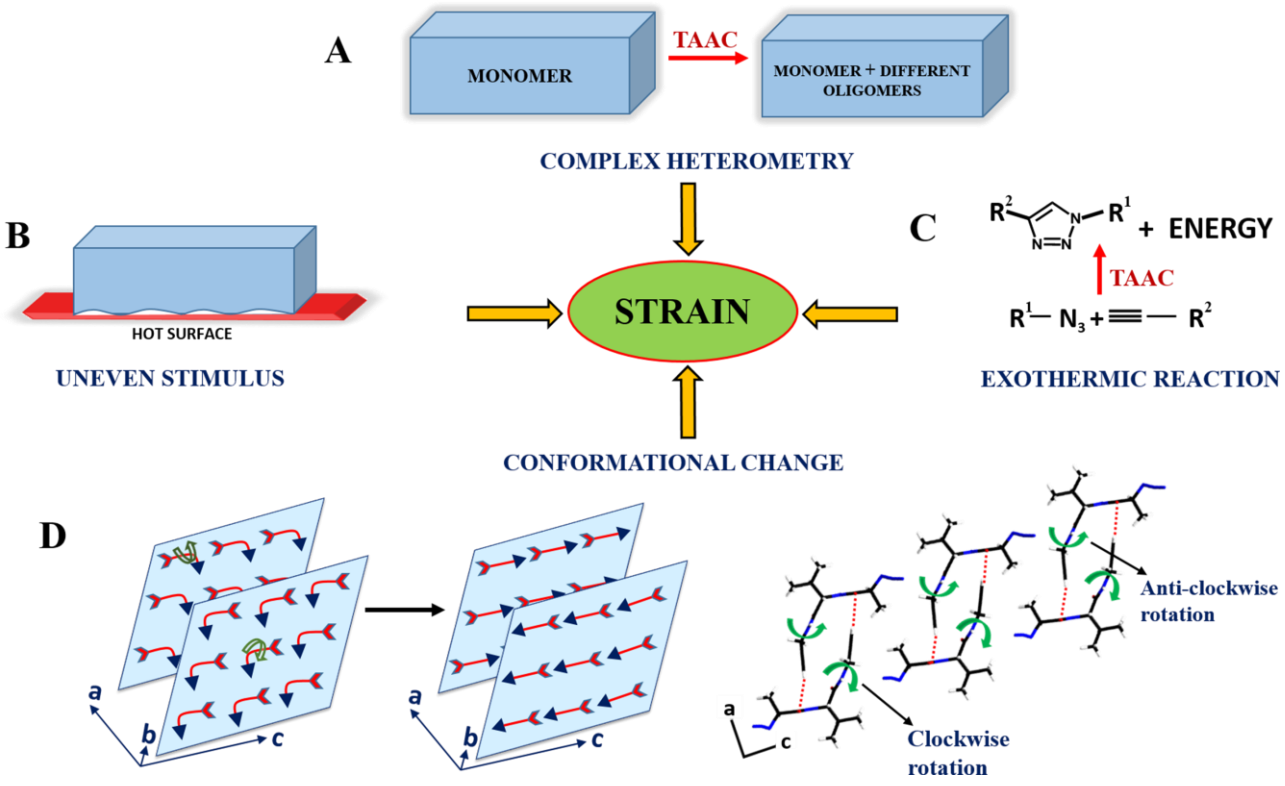

Fig. S9: Plausible factors that contribute to the overall strain in the crystal.

(B) Williamson-Hall (W-H) analysis of lattice strain

By analyzing the time dependent powder XRD spectra for dipeptide **LL** crystals (heated at 85 °C to undergo TAAC reaction) (3), W-H strain analysis has been done by using the following equation:

$$\beta_L^2 = \left(\frac{0.9\lambda}{a\cos\theta}\right)^2 + (4b\tan\theta)^2 + c^2$$

where, β_L = total broadening, λ = wavelength, θ = diffraction angle, a = particle size, b = lattice strain, c = instrumental broadening

It was observed from the PXRD that some peaks were intact in their sharpness throughout whereas others were broadened with time. Relative change in the strain has been studied by considering various peaks belonging to different set of (*hkl*) values. FWHM (full width at half maximum; β_L) values were obtained for all the peaks by peak fitting (using Pseudo-Voight function). These values were further subjected to the above equation to get the strain. At 0h, all the peaks were considered

for free fitting (Fig. S8) to get the values of *a*, *b* and *c*. The values of *a* and *c* thus obtained (9.448 x 10^{-10} and 0.006 respectively) were used in further calculations.

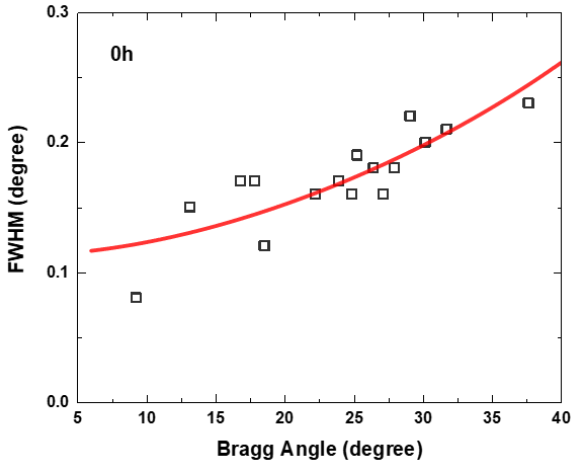

Fig. S10: Free fitting at 0h to get the values of *a* and *c* by taking into account all the peaks corresponding to different *hkl* values.

To monitor the change in strain with the progress of the reaction, set of peaks intact throughout were only considered.(Fig. S9). The variation of relative strain with progress of reaction revealed that the system has some existing strain which was enhanced further once the reaction starts (2%, 5% and 18% at 7h, 10h and 24h respectively) upon heating. The crystals thus twist in response to release this strain.

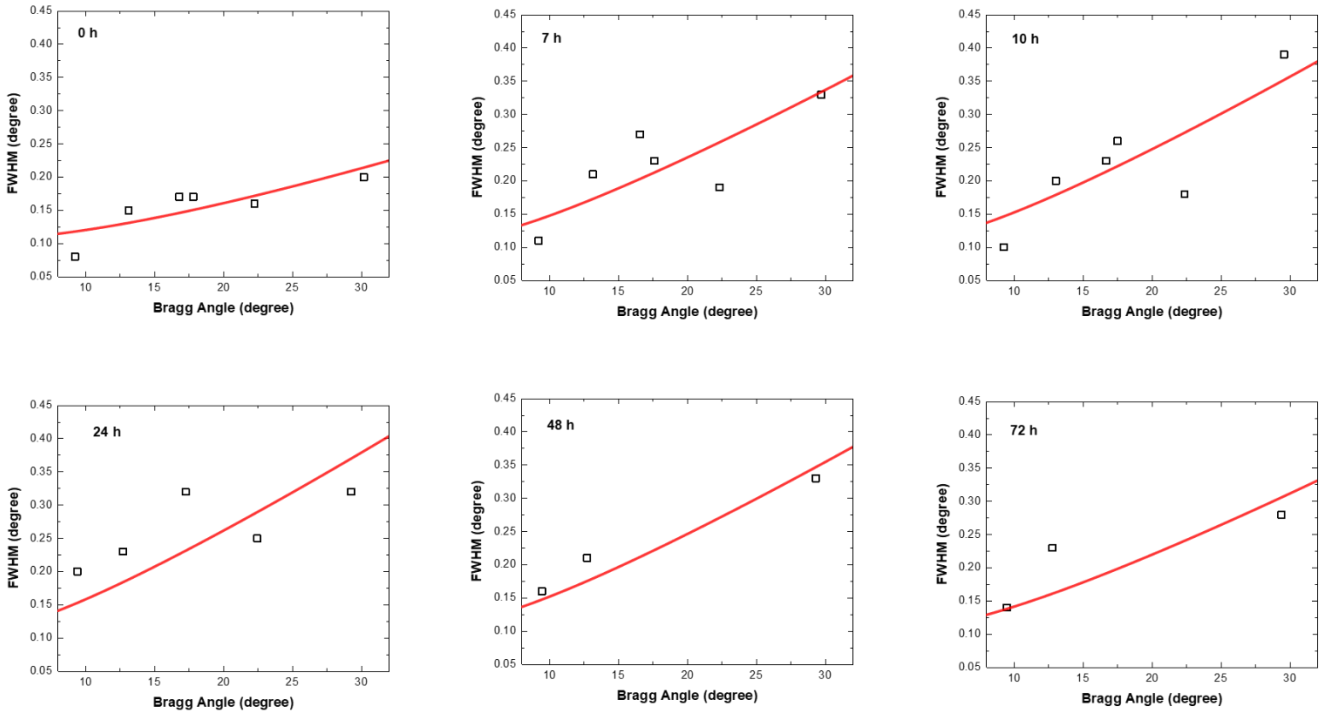

Fig. S11: Plot obtained at different time interval for selected set of peaks which are intact throughout. Peaks getting broadened with time are not considered.

S10. Synthesis and crystallization of dipeptide DD

The dipeptide **DD** was synthesized by following the procedure reported for the synthesis of **LL**.[S2] Dipeptide **DD** was crystallized from DCM/toluene mixture (3:1 v/v) by slow evaporation. Various crystallization techniques like solvent diffusion, floating drop, temperature dependent, slow evaporation etc. have been tried to obtain uniform crystals. Thin plate like crystals of variable sizes were obtained only by slow evaporation technique. All other methods resulted into formation of crystalline fibers even after several attempts of crystallization and re-crystallization. Crystals used for all studies were cherry-picked under polarizing microscope using very fine needle from different batches of crystallization.

^{1}H NMR (DMSO-d6, 500 MHz) δ: 8.50 (t, J = 5.5 Hz, 1 H), 8.20 (d, J = 8.8 Hz, 1 H), 4.15-4.12 (m, 1 H), 4.01 (q, J = 6.7 Hz, 1 H), 3.89- 3.83 (m, 2 H), 3.10 (t, J = 2.4, 1 H), 1.97-1.92 (m, 1 H), 1.31 (d, J = 6.7 Hz, 3 H), 0.85 (t, J = 6.9 Hz, 6 H). ^{13}C NMR (125 MHz, DMSO-d_6) δ: 170.85, 170.47, 81.36, 73.42, 58.03, 56.99, 31.20, 28.24, 19.49, 18.56, 17.00. $[\alpha]_D^{25}$ - 9.0° (*c* 0.10, methanol) (in contrast with $[\alpha]_D^{25}$ + 9.0 (*c* 0.10, methanol) for **LL)**.

Anal. Calcd for $C_{11}H_{17}N_5O_2$: C, 52.58; H, 6.82; N, 27.87. Found: C, 52.71; H, 6.86; N, 28.99.

S11. Single crystal XRD analysis of dipeptide DD

Crystallographic data are tabulated in Table S1, showing that **DD** also crystallized in monoclinic C2 space group (CCDC 1527669) similar to its enantiomer **LL**.

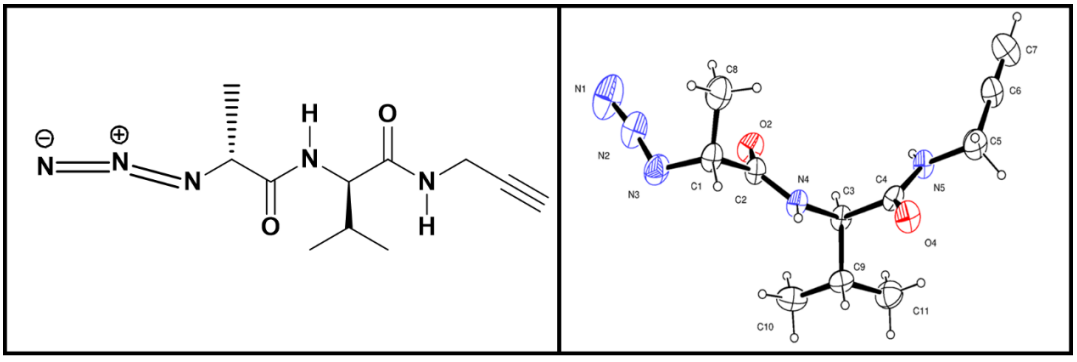

Figure S12. Chemical structure and ORTEP diagram of dipeptide **DD**.

Temperature (K)	296
Crystal system	Monoclinic
Space group	C2
Z	4
Z′	1
Absorption coefficient (mm^{-1})	0.086
Formula weight	251.29
a (Å)	28.39 (4)
b (Å)	4.831 (7)
c (Å)	10.611 (12)
α (degree)	90.000
β (degree)	107.47 (7)
γ (degree)	90.000

Cell volume ($Å^3$)	1388 (3)
ρ_{calcd} (g/cm^3)	1.202
λ (MoK_α) (Å)	0.71073
Collected reflns	4276
Unique reflns	2076
Goodness-of-fit on F2	0.999
Final R indices [I>2sigma(I)]	R1 = 0.1076, wR2 = 0.2479
R indices (all data)	R1 = 0.2402, wR2 = 0.3446

Table S1: Crystallographic data of dipeptide **DD**.

S12. Proof for TAAC reaction shown by crystals of dipeptide DD

In order to attain the parallel orientation of the azide and alkyne motifs, the molecules undergo rotation.

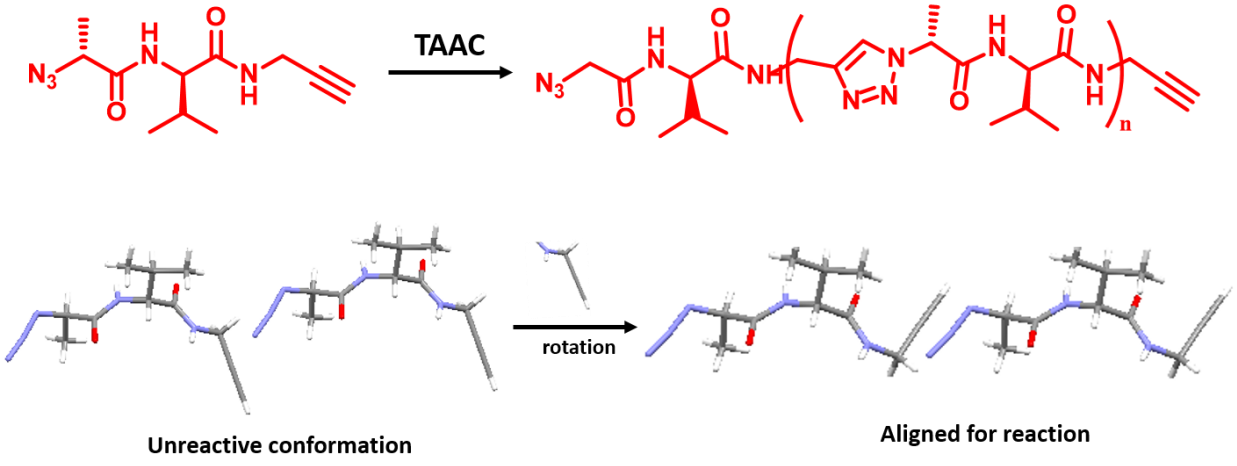

Fig. S13. Crystal packing arrangement of **DD** showing preferred orientation for reaction.

(A) ^{1}H NMR

Crystals of dipeptide **DD** were heated at 80 ˚C and portions were withdrawn at regular intervals of time and characterized by ^{1}H NMR spectroscopy after dissolving in DMSO-d6. The gradual progression of TAAC reaction forming 1,4-triazole linked oligopseudopeptides of D-aminoacids could be seen as in the case of dipeptide **LL** which gave 1,4-triazole linked oligopseudopeptides of L-aminoacids.

(B) IR study

IR spectra of both fresh crystals of **DD** and the heated crystals (at 80 ˚C for 7 days) were recorded. The relative intensity of azide stretching band (2103 cm^{-1}) was found to be reduced in the IR spectrum of the heated crystals. This showed the consumption of azide *via* topochemical polymerization as in the case of **LL** (Fig. S11).

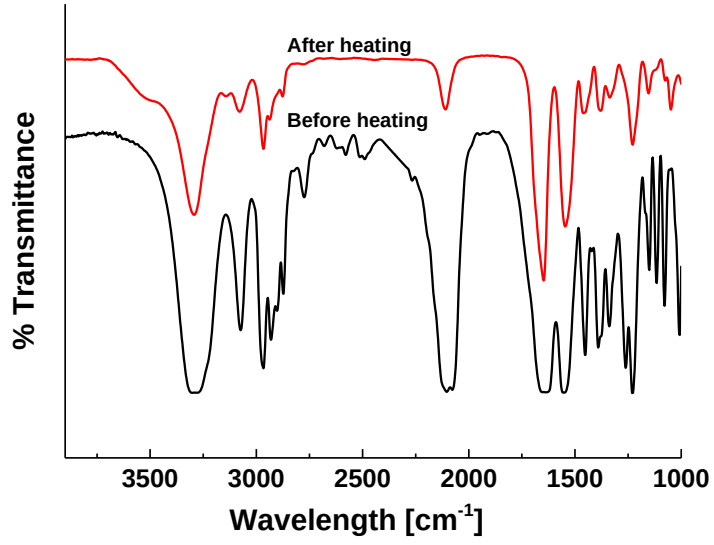

Fig. S14. IR spectral comparison of fresh crystals of **DD** and heated crystals (for 7 days at 80 ˚C).

(C) PXRD analysis

The PXRD pattern obtained for fresh and heated crystals of **DD** suggested that the crystallinity was maintained during the entire period of topochemical polymerization, indicative of the reaction proceeded in crystal-to-crystal fashion as in the case of **LL.**

(D) DSC experiment

Exothermic peak at 154 ˚C due to the uncontrolled Huisgen reaction was found to be vanished in the pre-heated crystals. This suggests that most of the azide and alkyne are consumed in the pre-heated crystals (Fig. S12).

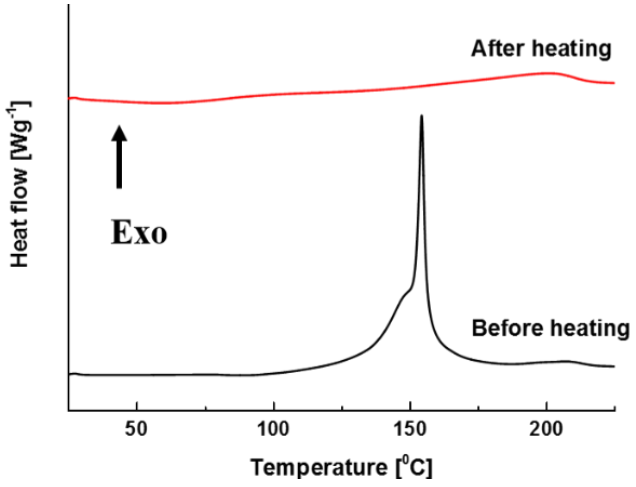

Fig. S15. DSC profiles of fresh crystals of **DD** and crystals heated for 7 days at 80 ˚C.

(E) MALDI-TOF spectrum

After heating for 7 days, **DD** crystals were found to be insoluble in all solvents due to the formation of higher oligomers upon reaction. MALDI-TOF spectrum recorded for the soluble portion of heated crystals in DMSO showed peaks corresponding to various oligomers, starting from dimer. Upto 12-mer was found to be present. As the length of chain increases, solubility decreases which attributes to decrease in the peak intensity of higher oligomers.

S13. Macroscopic chirality discrimination by molecular chirality

To check the role of molecular chirality in macroscopic morphological change (i.e. change in the twisting direction), we have heated a crystal of **LL** and **DD** together at 85 ˚C and viewed under polarizing light microscope. It is interesting to note that crystal of **LL** and **DD** twisted in right-handed and left-handed manner respectively suggesting that twisting direction is controlled by the inherent molecular chirality of dipeptides (Fig. S13-14).

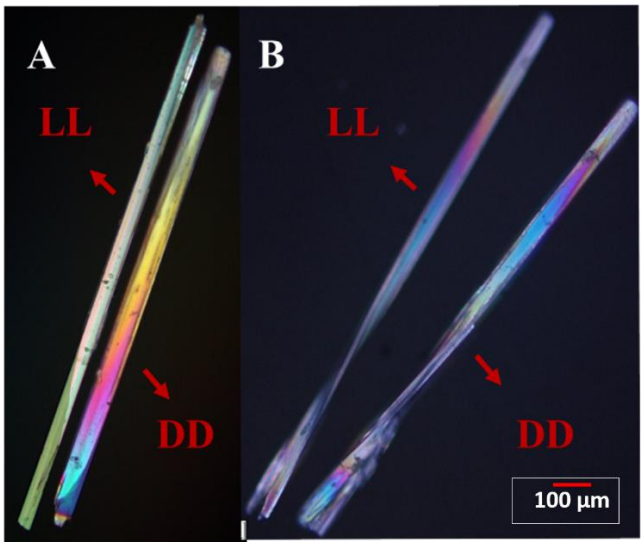

Fig. S16. Optical microscopic images (with polarizer) of crystal of **LL** and **DD** before (A) and after (B) heating at 80 ˚C for 24 h.

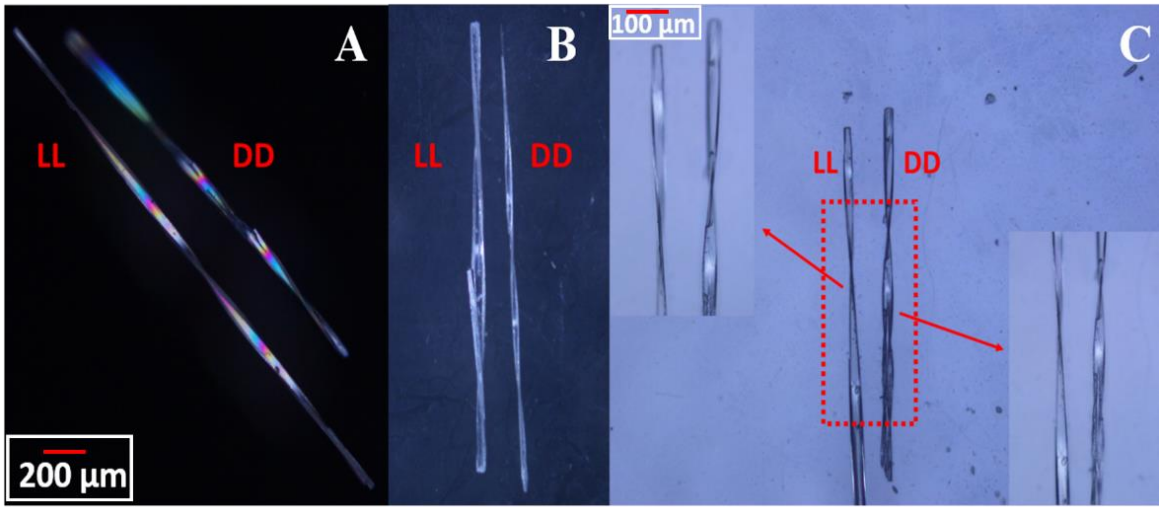

Fig. S17. Optical microscopic images of different sets of **LL** and **DD** crystals after heating at 80 ˚C for 72 h showing opposite handedness in twisting. (A) With polarizer; (B) with out polarizer; (C) with out polarizer. Portions of the images are magnified for clarity.

S14. Effect of the dimensions of crystals on twisting

Several crystals of variable dimensions were chosen and kept for uniform heating at 85 °C for 4 days in the oil bath. While monitoring the crystals regularly with time (using optical polarization

microscope), it was found that different crystals showed different number of twists. Smaller crystals form single twist whereas longer crystals form two to three twists (Table S2). We have also monitored the extent of twisting for a particular **DD** crystal (2.7 mmx 0.05 mm) with the time of reaction (uniform heating at 85 °C). Is is observed that at first the crystal showed slower rate of twisting. As time proceeded, the extent of twisting also increased significantly (plot shown in Fig. S19).

Table S2. Collection of different size crystals of dipeptide **DD** and **LL,** forming different no. of twists upon heating at 85 °C for 4 days.

Size of crystals (mm)	**No. of twists**	**Size of crystals (mm)**	**No.of twists**
1.83 x 0.04 (DD)	3	1.34 x 0.04 (LL)	3
1.76 x 0.05 (LL)	2	1.36 x 0.05 (LL)	2
1.60 x 0.05 (DD)	2	0.80 x 0.06 (LL)	1
1.03 x 0.05 (DD)	1	1.28 x 0.02 (LL)	3
1.10 x 0.04 (LL)	1	1.50 x0.02 (LL)	1
1.70 x 0.04 (DD_	3	0.85 x 0.05 (LL)	1
2.40 x 0.04 (LL)	3	1.40 x 0.05 (DD)	1
1.34 x 0.04 (DD)	1	1.27 x 0.05 (DD)	2
1.43 x 0.04 (LL)	1	2.66 x 0.05 (DD)	3

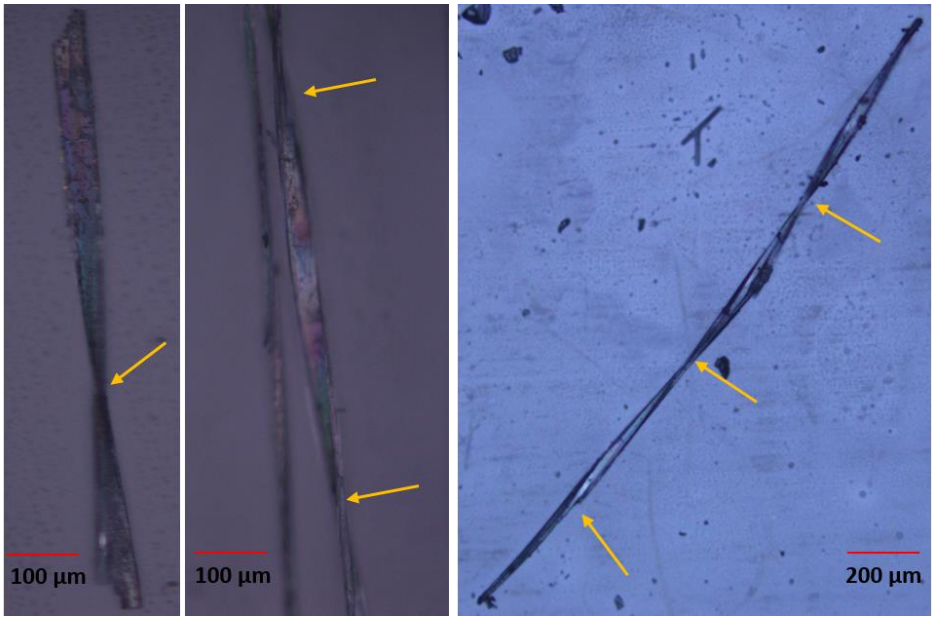

Fig. S18. Optical polarization microscopic images of different size crystals forming different no. of twists (one, two and three respectively) upon heating at 80 °C.

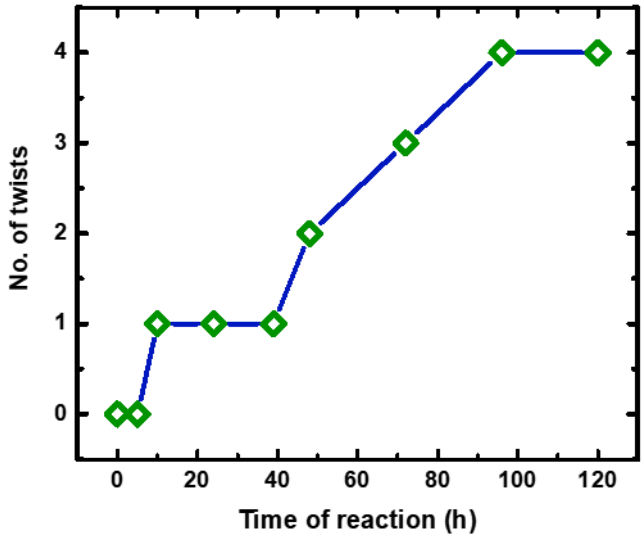

Fig. S19. Plot correlating the extent of twist for a particular **DD** crystal (dimension 2.7 x 0.04 mm) with time of reaction progress.

S15. Estimation of energy needed for the twisting of crystals

To approach the quantitative side of this phenomenon, we have attempted the calculation of energy required for twisting these crystals (4). Considering the observation that the required energy to twist a crystal (τ = shear stress) can be estimated by using the following equation:

$$\tau = \frac{E\theta\sqrt{ab}}{4h(1+\upsilon)\sqrt{\pi}}$$

where, crystals under study are considered to be plastic in nature having E = Young' s modulus (15 GPa, 5), θ = angle of twist (in radian), υ = Poisson's ratio (taken as 0.0 and 0.5 to calculate the range of energy, 6), $a \times b \times h$ = dimension of crystal.

Four sample crystals representing the over all size range of the crystals under study were chosen. The energy required to twist these crystals by 180° (kJ/mol) has been calculated (Table S3). As organic crystals show positive Poisson's ratio from 0-0.5, we have calculated the energy with these boundary values. Also the energy values have been calculated to twist these crystals from 0 to 360° at each 1° intervals (Fig. S16). The variation in the slope of the plots of twist-angle vs energy for crystals of different dimensions is in accordance with the experimental trend. The maximum energy (υ = 0) required for twisting the sample crystals by 360° fall in the range 34.5 to 62.8 kJ/mol.

Table S3. Energy required to twist dipeptide crystals (**DD** and **LL**) of variable dimensions (calculated at υ = 0.5 and 0.0).

Sample crystal's size (mm)	**Energy requied for 1 twist (180°) (kJ/mol)**	
	υ = 0.5	υ = 0
1.03 x 0.05 x 0.01 (DD_1)	20.9	31.4
1.10 x 0.04 x 0.01 (LL_2)	17.4	26.3
1.43 x 0.04 x 0.01 (LL_3)	13.4	20.3
2.35 x 0.04 x 0.02 (LL_4)	11.5	17.3

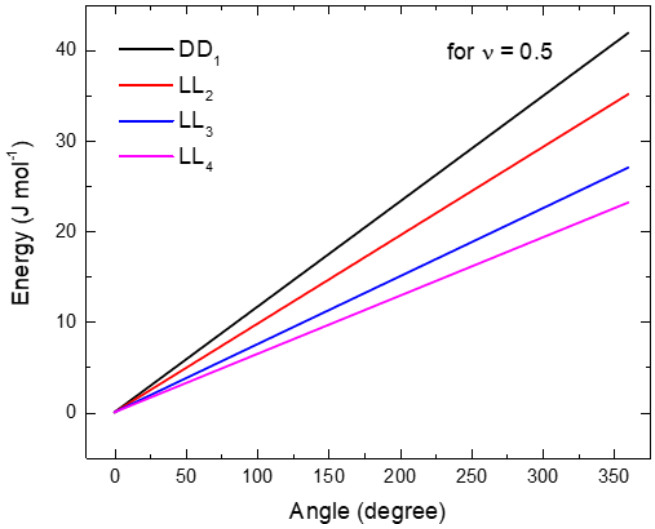

Fig. S20. Plot of energy (at υ = 0.5) versus angle of twist of various dipeptide crystals (**DD** and **LL**) having different sizes.

S16. Spectra

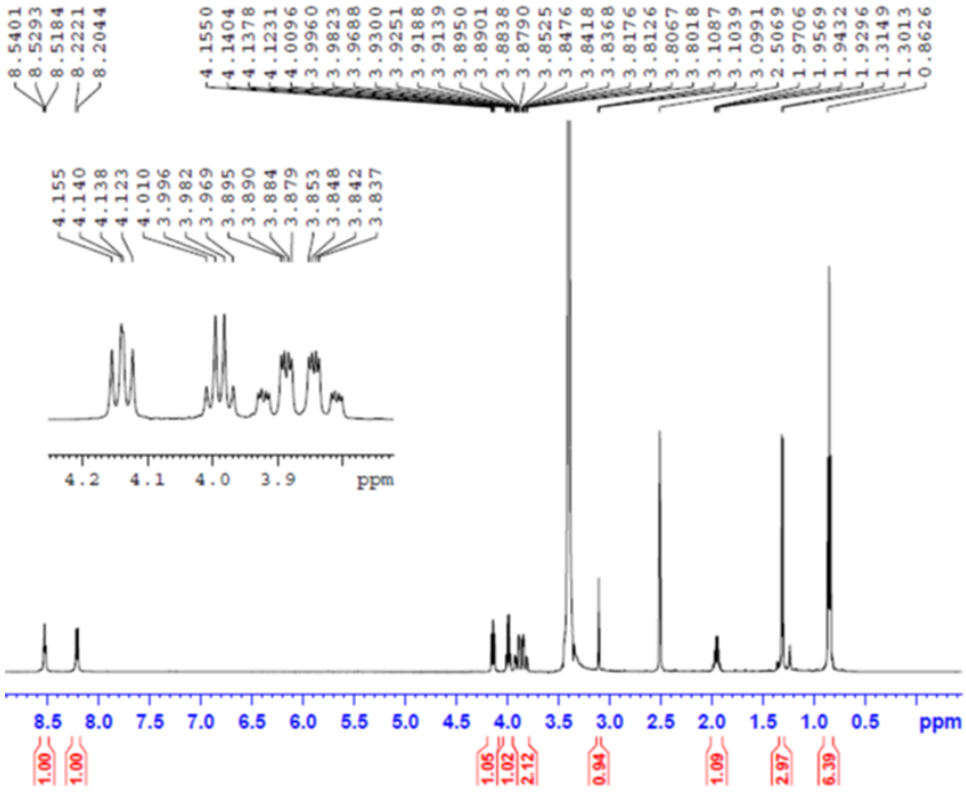

Fig. S21. ^{1}H NMR spectrum of dipeptide **DD**.

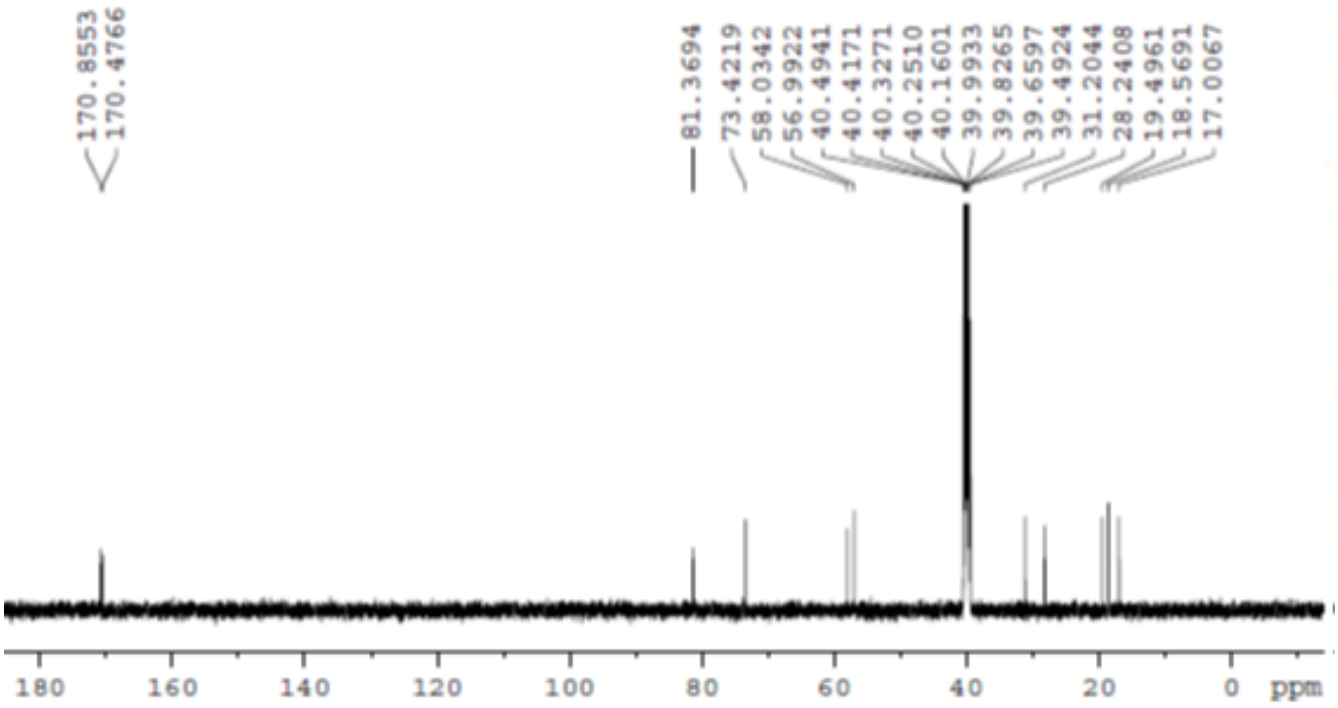

Fig. S22. ^{13}C NMR spectrum of dipeptide **DD**.

(A)

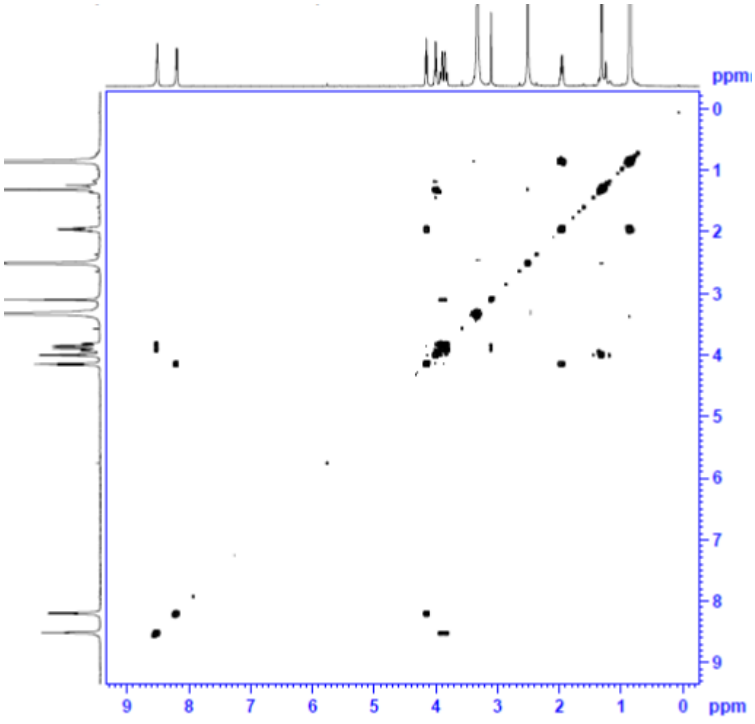

(B)

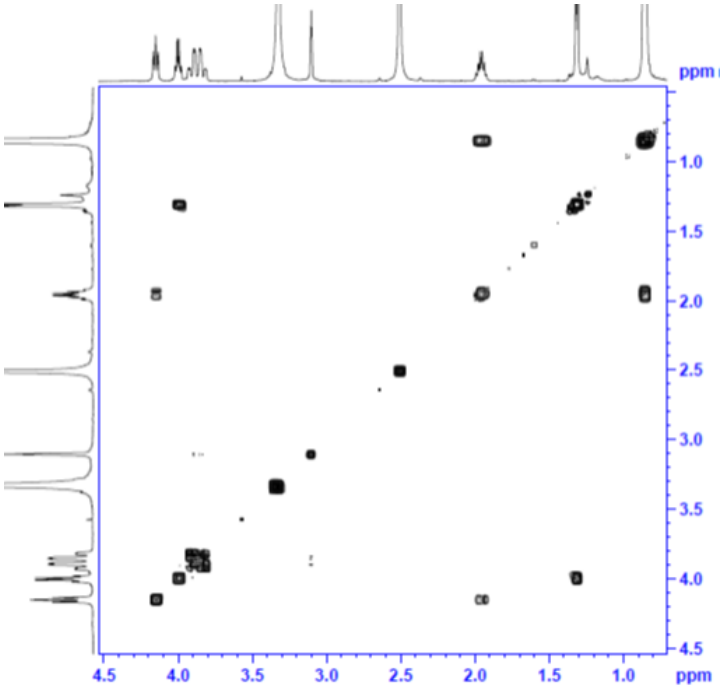

Fig. S23. (A) COSY spectrum of dipeptide **DD**; (B) Zoomed spectrum

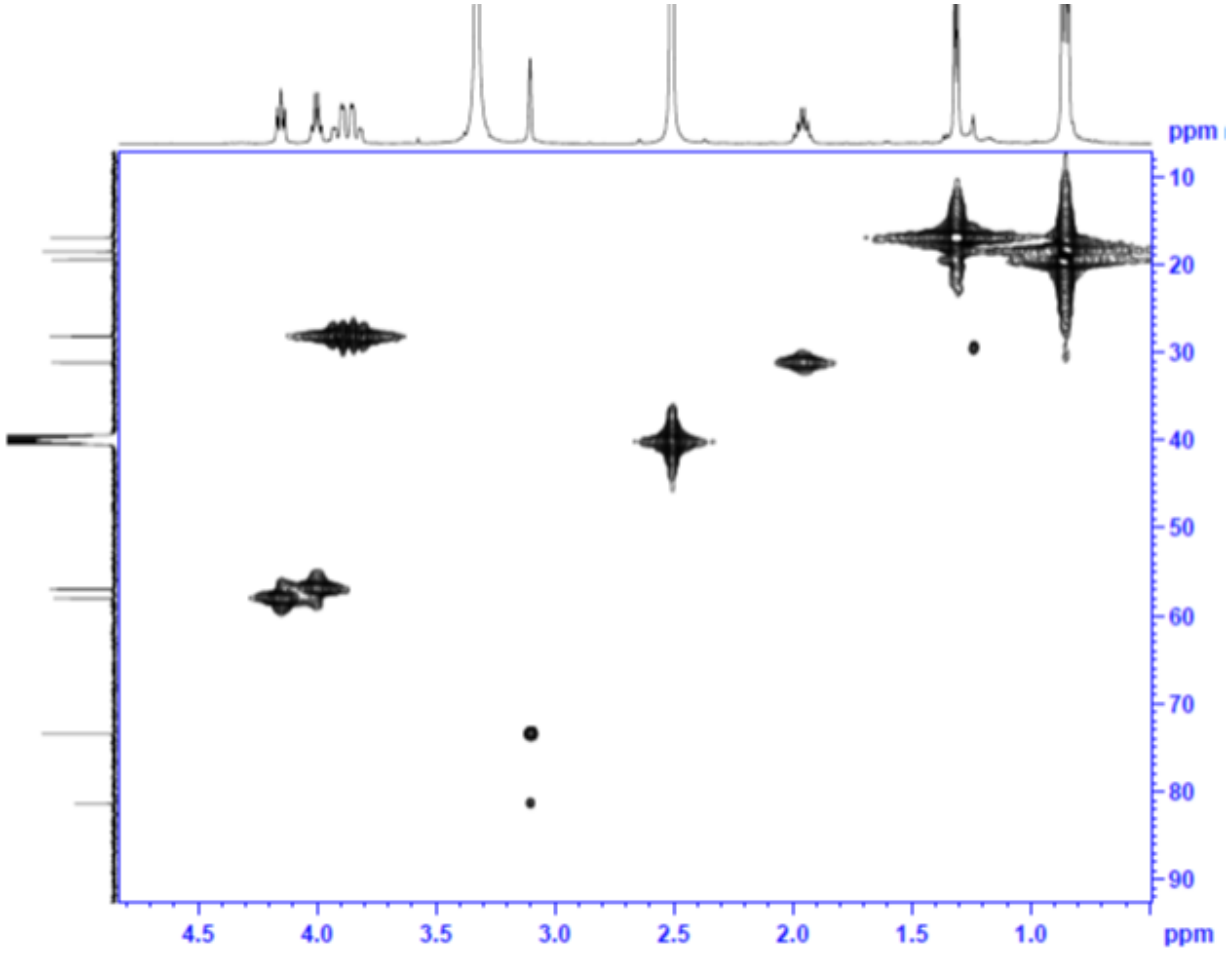

Fig. S24. HMQC spectrum of dipeptide **DD**.

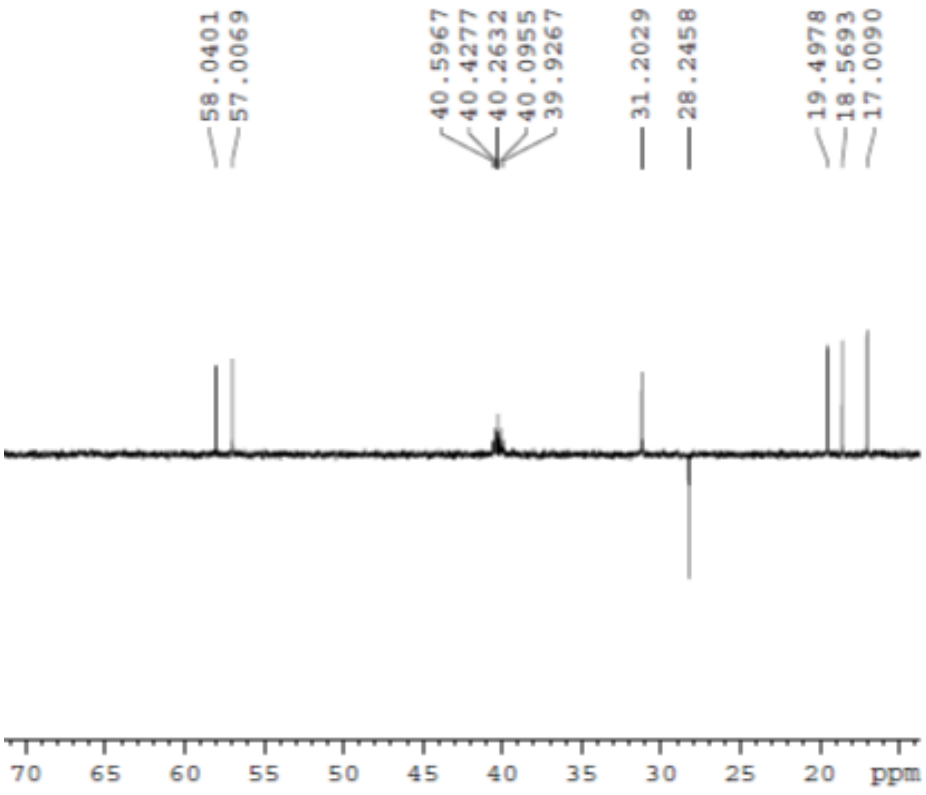

Fig. S25. DEPT spectrum of dipeptide **DD**.

S17. References

1. Zhou y, Guo W, Cheng WJ, Liu Y, Li J, Jiang L (2012) High-Temperature Gating of Solid-State Nanopores with Thermo-Responsive Macromolecular Nanoactuators in Ionic Liquids. *Adv Mater* 24: 962-967.

2. Naumov P, Chizhik S, Panda MK, Nath NK, Boldyreva E (2015) Mechanically Responsive Molecular Crystals. *Chem Rev* 115: 12440-12490.

3. Krishnan BP, Rai R, Ashokan A, Sureshan KM (2016) Crystal-to-Crystal Synthesis of Triazole-Linked Pseudo-proteins via Topochemical Azide–Alkyne Cycloaddition Reaction. *J Am Chem. Soc* 138: 14824-14827.

4. Saha S, Desiraju GR *J Am Chem Soc* 139: 1975-1983.

5. Zhu L, Al-Kaysi RO, Bardeen CJ *J Am Chem Soc* 133: 12569-12575.

6. Ashby MF, Jones DRH (1980) *Engineering Materials*, Pergamon, Oxford 31.